Influence of Active Antennas on EMF Restrictions in 5G Base Stations Deployment

Sofia D. Patrício, Luís M. Correia and Mónica A.M. Gomes

***Abstract*— This thesis aims to develop a model to analyse the influence of active antennas on electromagnetic field restrictions in 5G base stations deployment. The model allows for the computation of electromagnetic exposure in the vicinity of base station antennas with 3.6 GHz in order to compute the respective exclusion zone that guarantees the safety of the population. The electric field is estimated as a function of distance for a Huawei antenna, using the CST Studio Suite simulation software. In order to avoid overestimated results, the active behaviour of the antennas is taken into account, considering realistic maximum power levels. Later, multi-band exposure is determined in order to define appropriate exclusion zones and analyse the impact of 5G installation on the increase of the existing exclusion zones, created by the legacy systems. This analysis allows for the evaluation of whether and under what conditions the increase in the exclusion zone requires the definition of physical barriers. Representative scenarios with co-location of antennas are analysed. First, the compliance distance considering only the exposure from the 3.6 GHz is determined, then, the exclusion zone distance before and after the installation of both 5G bands (700 MHz and 3.6 GHz) is computed. The highest increase in the exclusion zone distance is 170.4%, 78% and 104.1%, for urban, suburban and rural scenarios, respectively. The obtained results support that, in some scenarios, operators may need to reduce the total transmitted power in order to ensure the safety of the population.**

***Index Terms*—Electromagnetic field, 5G, Exclusion Zone, Time-average, Near-field.**

I. Introduction

The evolution of cellular communication networks has been happening since the early 1980s. Almost every ten years, a new generation of mobile communication networks appears, each one of them being more powerful than the previous one, presenting new features, techniques and capabilities.

The 5th generation of mobile networks (5G), known as New Radio (NR), constitutes the newest step in telecommunications. With 5G, broadband wireless services are taken to another level, ceasing to stick only to the mobile internet and starting to move towards the Internet of Things (IoT) and more critical communication scenarios. This generation allows for massive connectivity among people, among machines and between each other [1]. With larger bandwidth, 5G can use shorter frequencies (millimetre waves range), offering a maximum speed of 10 Gbps, about 10 to 100 times faster than 4G. With such a high-band spectrum, it is possible to increase the speed and decrease latency, achieving a low value of 1 ms. When compared to 4G, capacity has increased up to 100 times the number of connected devices per unit area, with 99.999% availability and improved coverage, and a 90% reduction in network energy usage [2].

Despite these accomplishments, the arrival of 5G raised some concerns about the exposure to Radiofrequency (RF) Electromagnetic Fields (EMFs), which may have negative health effects on people. The high data rates required by 5G imply higher signal power at the receiver, raising concerns about the amount of radiation applied to the user. With 5G, Base Stations (BSs) will operate with more transmitters and narrower beams. Smaller cellular networks will be used to provide service for smaller areas. Thus, with the antennas being located closer to users, the chances of human exposure to radiation from EMFs may increase. In order to ensure the safety of citizens, there are entities in charge of establishing guidelines for limiting exposure to EMFs, such as the International Commission on Non-Ionising Radiation Protection (ICNIRP).

Besides the licenced spectrum below 6 GHz, 5G is foreseen to use spectrum above 6 GHz (millimetre waves range). However, sub-6GHz is the candidate for early deployment networks, so for the following years, the application of 5G will be predominantly for frequencies in the bands of 700 MHz and 3.6 GHz, which are the bands taken for this thesis. While the 700 MHz band facilitates the transition to 5G and coverage in different areas, the 3.6 GHz band is responsible for providing the necessary capacity for services supported on 5G systems.

Due to the deployment density of 5G networks and a notable reduction in the distance between the users and the antennas, the usual estimation of EMF radiation distribution in the far-field zone will not be enough. The current methodology for determining EMF exposure assumes that the transmitting antennas have predictable radiation patterns and that the BS is transmitting signals at its theoretical maximum power. However, these assumptions should not be made when using

S.D. Patrício, Master Student, Instituto Superior Técnico, University of Lisbon, Av. Rovisco Pais, 1049-001 Lisboa, Portugal (e-mail: sofia.patricio@ist.utl.pt)

L.M. Correia, Professor, Instituto Superior Técnico – INOV/INESC, University of Lisbon, Av. Rovisco Pais, 1049-001 Lisboa, Portugal (e-mail: luis.correia@inov.pt).

M.A.M. Gomes, Engineer, Huawei Technologies Portugal Lda, Av. Dom João II 118 Block 10A, 1998-028 Lisboa, Portugal (e-mail: monica.Gomes@huawei.com).

massive Multiple Input Multiple Output (mMIMO) and beamforming, making the existing measuring methods not suitable for NR antennas.

In [3], a statistical approach for the computation of EMF, considering MIMO systems and exploiting narrow beams, is provided. By taking a three-dimensional (3D) spatial traffic model into account, it was possible to conclude that the exclusion zone is approximately half of the one in the traditional case, based on the maximum radiated power in all directions.

In [4], a model to compute realistic maximum power levels of 5G BSs with mMIMO is proposed. Results have shown that the time-averaged radiated power is approximately between 7% and 22% lower than the maximum theoretical one, which can be translated into a reduction of the distance from the antenna to the compliance limit up to 60% compared with the more common evaluations.

In [5] and [6], an analysis of the actual power and EMF exposure from BSs with mMIMO antennas in a commercial 5G network is done. The results end up being highly influenced by the surrounding environment and software limitations since they are based on actual measurements. While an exclusion zone is only determined in the second work, both of them make several assumptions and simplifications, affecting the results. However, the final results are consistent with those presented in other works.

Finally, in [7], an analysis of the impact of EMF restrictions on 5G BSs deployment in the existing network is done. A model for estimating the exclusion region of a BS is proposed, which estimates the power density as a function of distance for each mobile communication system and any given direction, using far-and near-field mathematical models and considering that the antennas are continuously radiating at maximum power. Taking representative scenarios of BSs with co-location of antennas, an analysis on the exclusion zone distance is made before and after the installation of NR. The obtained results show that, for the urban scenarios, the highest increase is 248.7%, while, for the suburban and rural scenarios, it is 131.6% and 56.4%, respectively. These results support that, in some cases, there may be a need to reduce the power transmitted in order to comply with the restrictions. However, this work is based on the worst-case scenario since it is assumed that the antennas are continuously radiating at maximum power.

The main goal of the present work is to develop a model to determine EMF exposure in the vicinity of BS antennas with 3.6 GHz NR installed in order to compute the respective exclusion zone that guarantees general public safety. The development of the model takes the active behaviour of the 3.6 GHz NR antennas into account by considering realistic maximum power levels, leading to less overestimated results.

This paper is composed of 5 sections, including the present one. In section II, EMF radiation exposure around a BS with the respective international safety established guidelines and definition of an exclusion zone are addressed. In section III, the methodologies for the development of the model are presented, along with an overview of the general model. In section IV, an analysis of the results obtained from the model is presented. Finally, in section V, the main conclusions of the thesis are summarized, along with some suggestions for future work.

II. Fundamental Aspects

A. EMF Radiation Exposure

ICNIRP has established guidelines for limiting EMF exposure, providing a high level of protection against adverse health effects [8].

In order to facilitate the evaluation of EMF radiation, reference level quantities were defined, such as the incident electric field strength, E_{inc}, magnetic field strength, H_{inc} and power density, S_{inc}. The reference levels for E, H and S have been derived from studies assuming whole-body exposure to a uniform field distribution, which is generally the worst-case scenario.

The averaging time must also be taken into account since this is the time over which exposure is averaged for purposes of determining compliance. The most commonly used ICNIRP reference levels for exposure are the ones averaged over 6 min and 30 min. However, it is possible to determine reference levels for exposure for lower averaging times by using the incident energy density, U_{inc}, reference levels for local exposure, integrated over intervals of between 0.5 min and 6 min. These values can be useful when investigating EMF exposure in scenarios where the average service duration is less than 6 min [8].

B. Exclusion Zones

There are some regions near the antenna, usually some metres within the near-field region of the BS, where human exposure limits are known to be well exceeded, which are usually positioned around antennas on rooftops in urban or suburban scenarios. These regions should be physically delimited or signalled in order to protect the general public from radiation exposure, unless they are on masts, especially in rural scenarios, in an area that is not accessible to the general public.

The radiated field behaviour is not the same for each of the three regions surrounding an antenna (reactive near-field region, radiating near-field region and far-field region), hence the importance of accurate propagation models to estimate the exact field strength at any given distance. For typical radiated power values and antenna dimensions, the field at the minimum far-field distance is below the recommended values [9]. However, it is essential to guarantee improved near-field propagation models for the estimation of the exclusion zones. Based on [9], an exclusion zone can be defined as a cylinder with, D_{front}, D_{back}, D_{side}, D_{top} and D_{bottom} distances.

III. Model Development and Implementation

A. Model Overview

A representation of the model configuration is presented in Figure 1.

Since the goal of this thesis is to determine time-averaged realistic maximum power levels, it is necessary to estimate the temporal variation contribution to exposure, T_{var}, taking users' mobility and services' characteristics into account. Therefore, a time behaviour model was developed in order to estimate the duration of a service and an antenna beamforming model was developed to estimate mobility, distinguishing user's movement. Then, the general model for estimating exclusion zones around a BS was developed, taking the EMF exposure

assessment model and the previous estimation of T_{var}. Since regulation is based on the total exposure of a site, the variation of the exclusion zone when an NR antenna is installed in a BS with GSM, UMTS, and LTE technologies must be determined. Thus, the exclusion zone distance needs to be computed before and after the installation of the NR antenna.

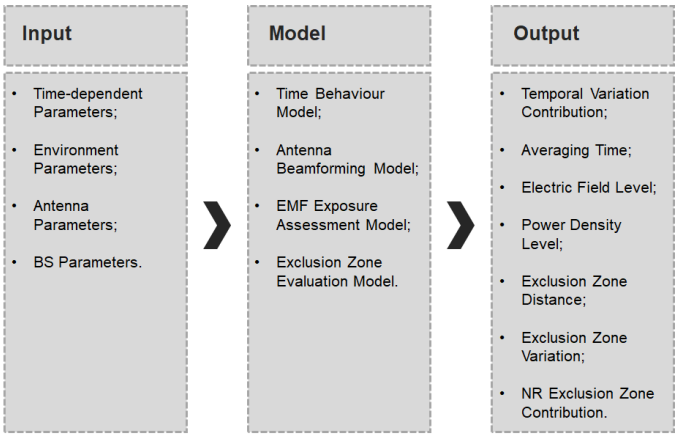

Figure 1. Model configuration (based on [7]).

The inputs for the model can be divided into four categories: time-dependent parameters, environment parameters, antenna parameters and BS parameters. Regarding the output parameters, seven different outputs can be estimated: the temporal variation contribution and the averaging time are the outputs from the first two models, becoming the drivers of the following ones. The temporal variation contribution is expected to generate smaller exclusion zones, since the actual power density is expected to be significantly smaller than the maximum one. The electric field and correspondent power density levels are computed, as a function of distance, in order to allow for the computation of the exclusion zone. The exclusion model is then able to compute the exclusion zone distance. Consequently, the exclusion zone variation and NR contribution may also be determined.

B. CST Simulation Software

In order to obtain a representation of the electric field strength as a function of distance, the 96 dual-polarized AAUxxxxw Huawei antenna [10] is simulated for the direction of maximum radiation using the CST Studio Suite software, a high-performance 3D electromagnetic analysis software [11].

A Time Domain solver was chosen, since it offers the largest simulation flexibility, while being very efficient for high frequency applications, such as the case under study. Furthermore, since the goal is to simulate a planar array antenna (considerably larger than the unit cell), the Frequency Domain solver, based on the Finite Element Method (FEM), is not the most adequate, since the numerical requirements scale exponentially with the size of the problem.

According to [12], for the case under study, the most adequate solver is the Transient one, based on the Finite Integration Technique (FIT). Unlike FEM, the numerical requirements of FIT scale linearly (the simulation time increases in the same proportion as the number of mesh cells), allowing for the simulation of larger problems using fewer computational resources in a shorter time.

First, the unit element of the planar array antenna (a half-wavelength dipole antenna) was designed with a radius, a, of 0.50 mm, an optimised Length, L, of 36.14 mm and a feed gap, g of 0.20 mm ($L/200$).

Since the size of the planar array is finite, it is necessary to take into consideration some non-periodic effects, such as the edge effects and other physical realities. Therefore, a simulation of the full array must be performed. Taking the specifications of the antenna into account, it is possible to define the desired planar array using the CST Array task.

By considering the elements equally spaced along the correspondent dimensions of the antenna, it is possible to approximately determine the horizontal and vertical distance between elements, d_{ele}^{H} and d_{ele}^{V}, being given, respectively, by

$$d_{ele}^{H} = 0.53\,\lambda, \tag{1}$$

$$d_{ele}^{V} = 0.67\,\lambda, \tag{2}$$

where λ is the wavelength of the transmitted electromagnetic wave.

A plane ground, composed of PEC material, must be added at a distance λ/4 from the dipole antennas [13], having the dimensions of the planar array antenna. The boundaries should be fixed to Open (add space) for all limits, except the z_{min}, which should be settled as Electric. One should note that, when adding the ground plane, the reflection coefficient will obviously change, however, for the scope of this thesis, this behaviour does not significantly affect the intended results. A design of the full planar array antenna is presented in Figure 2.

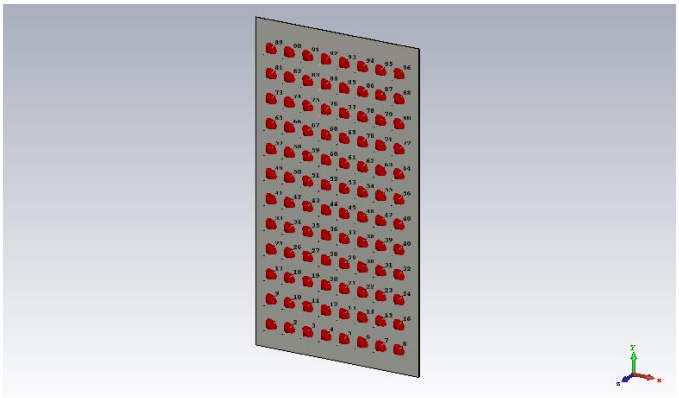

Figure 2. Design of the 8 × 12 planar array in CST, placed in the xOy plane.

Setting the frequency between 3.45 GHz and 3.7 GHz, the half-wavelength dipole is fed with a 50 Ω impedance and an input power of 1 W. Considering the mesh options, the hexahedral mesh type is chosen, with an accuracy of −40 dB. As chosen mesh properties, one has 15 Cells per Wavelength Near to Model and Far from Model, and 20 as the Fraction of Maximum Cell Near to Model, resulting in 113 256 mesh cells. The goal is to obtain the best trade-off between simulation speed and accuracy.

The 3D and two-dimensional (2D) E-pattern and gain far-field results for the AAUxxxxw antenna are represented in Figures 3, 4 and 5, respectively. In the 2D representations,

while the area outlined with red represents the radiation pattern, the light blue line corresponds to the 3 dB beamwidth, the green line to the -3 dB mark and the dark blue line to the direction of the main lobe, i.e., of maximum radiation.

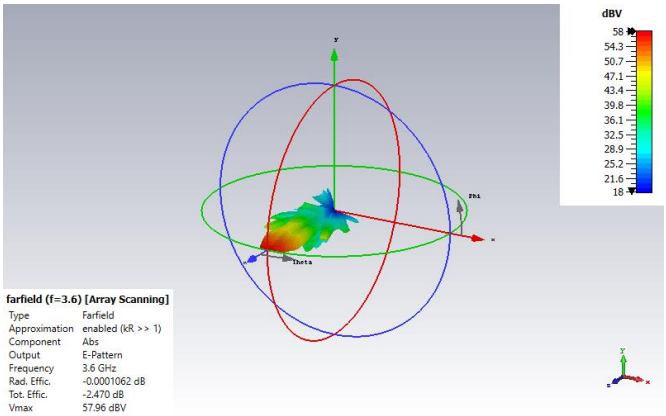

Figure 3. 3D 8 × 12 planar array E-pattern with ($\theta = 0°, \phi = 0°$).

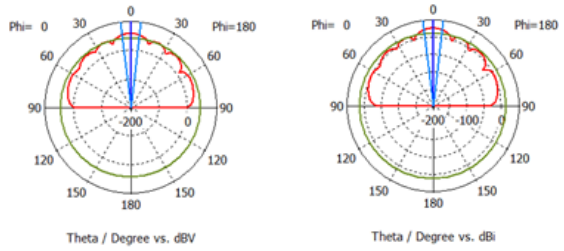

(a) Far-field E-pattern (b) Far-field Gain pattern

Figure 4. 2D far-field cut ($\phi = 0°$) of the electric field and gain patterns for the 8 × 12 planar array.

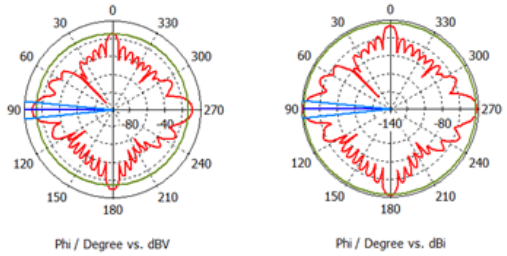

(a) Far-field E-pattern (b) Far-field Gain pattern

Figure 5. 2D far-field cut ($\theta = 90º$) of the electric field and gain patterns for the 8 × 12 planar array.

C. *Near-field Results*

Taking into account the dimensions of the antenna (730 × 395 × 160) [mm^3], the limit distance between the reactive near-field and radiating near-field is approximately 1.62 m while the Fraunhofer distance is approximately 16.54 m, based on the expressions presented in [13].

Given the goal of these experiments, one must focus on the near-field results between approximately 1.62 m and 16.54 m in order to determine whether the behaviour of the electric field in this region follows the expected theoretical behaviour, i.e., varies with distance according to [13]

$$E \propto \frac{C_{2[\mathrm{m}]}}{d_{t[\mathrm{m}]}^2} + \frac{C_1}{d_{t[\mathrm{m}]}} + C_{0[\mathrm{m}^{-1}]}, \quad (3)$$

where C_2, C_1 and C_0 are the fit coefficients.

By using the Evaluate Field on Curve option, it is possible to obtain the electric field strength as a function of distance in the near-field region. Since, in this case, the calculation domain will increase significantly, the mesh properties and accuracy must be adjusted in order to allow the simulations to run the with the available CPU and RAM. As chosen mesh properties, one has 10 Cells per Wavelength for Near to Model and Far from Model and 60 as the Fraction of Maximum Cell Near to Model. The latter guarantees that the excitation ports are located along the mesh edges. The accuracy is set at -30 dB, which is considered to be a moderate accuracy level. If there is still a certain amount of energy left in the structure when the solver stops, a truncation error will appear, causing some ripples in the S-parameter curves but not shifting the frequency of the pole. Because the location of the minimum is all that matters in this thesis, a larger truncation error is acceptable [12].

The electric field strength as a function of distance in the near-field region is represented in Figure 6.

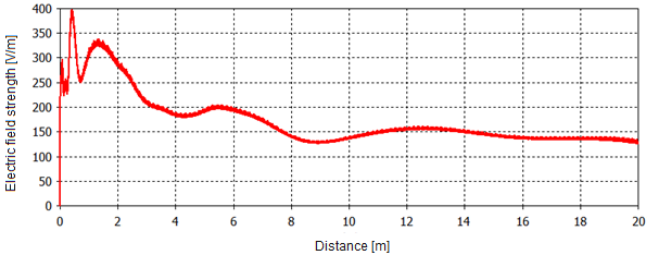

Figure 6. AAUxxxxw electric field strength decay with distance in the radiating near-field region.

With the obtained results, an overestimation of the electric field is performed, i.e., an interpolation is performed, based on the maxima of the electric field strength as a function of distance. It is then possible to verify the expected behaviour in (3) through a regression, obtaining as fit coefficients: $C_2 = -297.5$ m, $C_1 = 513.2$ and $C_0 = 123.1$ m^{-1}. Figure 7 shows the near-field data and the respective fitted curve.

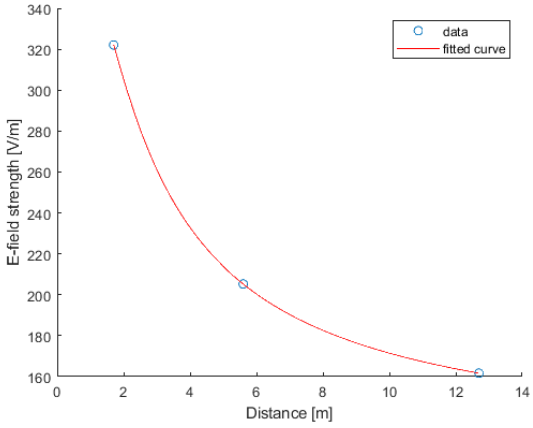

Figure 7. AAUxxxxw electric field strength decay with distance in the radiating near-field region.

Due to the high far-field region distances of the antenna under study, in order to determine the electric field values these distances with the Evaluate Field on Curve method, the resulting calculation domain would require an unavailable computational capacity. However, by using the Far-field Monitor tool, it is possible to conclude that the field decays proportionally to $1/d$, as expected. Therefore, given the behaviour of the field in the different radiating regions, it is possible to conclude that the limits between radiation regions seem to be according to the theoretical limits.

One should note that while C_2 and C_1 coefficients define the curvature of the curve, C_0 is only responsible for shifting of the plot in the y-axis. Therefore, C_2 and C_1 remain constant but C_0 must change according to the chosen far-field distance.

Taking into account the behaviour of the electric field in the far-field region, it is necessary to make some adjustments to the obtained near-field curve in order to guarantee a smooth transition to the far-field region. Hence, the electric field plot for the near-field region must be shifted by changing the coefficient C_0. Therefore C_0 must be determined according to

$$\frac{C_{2[\mathrm{m}]}}{d_{[\mathrm{m}]}^2} + \frac{C_1}{d_{[\mathrm{m}]}} + C_{0[\mathrm{m}^{-1}]} = \frac{1}{d_{[\mathrm{m}]}}\Big|_{d_{[\mathrm{m}]}=16.54}, \quad (4)$$

which results in a C_0 equal to -29.88 m^{-1}.

The plot contemplating the field behaviour in the radiating near-field and far-field region is presented in Figure 8.

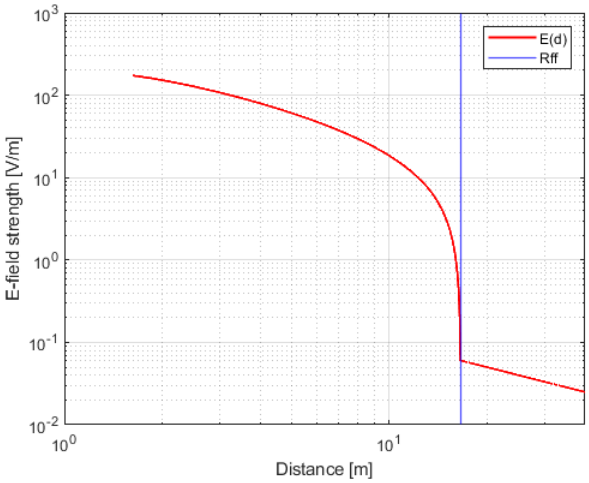

Figure 8. AAUxxxxw electric field strength as a function of distance for the radiating near-field and far-field region in a logarithmic scale.

D. Exclusion Zone Evaluation Model

Considering the obtained results, the general expression for the electric field strength can be given by

$$E(\theta,\phi,d)_{[\mathrm{V/m}]} \cong V_{M[\mathrm{V}]}\, f_{\theta\phi}(\theta,\phi)\, f_d(d)_{[\mathrm{m}^{-1}]}, \quad (5)$$

where V_M is the maximum voltage, $f_{\theta\phi}(\theta,\phi)$ is the normalised 3D antenna radiation pattern and $f_d(d)$ is the function representing the electric field dependency with distance.

The maximum voltage is given by

$$V_M = \sqrt{30\, P_{in}\, G_M}, \quad (6)$$

where P_{in} is the antenna input power and G_M is the maximum antenna gain.

The AAUxxxxw antenna gain patterns are represented in Figure 9, where the area outlined with the blue line corresponds to the maximum beam coverage scope, the one in red to the minimum beam coverage scope and the one in green to the area of actual operation of the antenna.

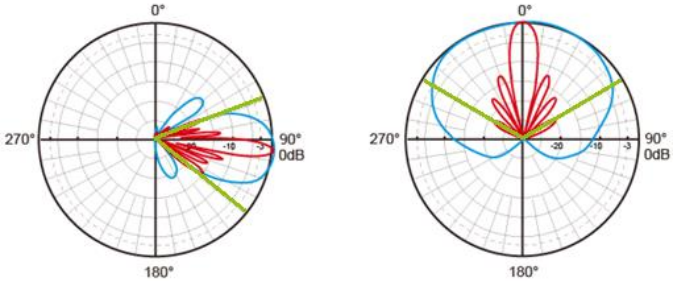

(a) Vertical radiation pattern (b) Horizontal radiation pattern

Figure 9. Vertical and horizontal radiation patterns of AAUxxxxw beams in a macro coverage scenario (adapted from [10]).

Taking into account the maximum beam coverage scope of the radiation patterns, the normalised 3D antenna radiation pattern can be determined by multiplying the normalised antenna radiation pattern in the vertical and horizontal plane (estimated by the observation of the radiation patterns of the antenna), along with the normalised antenna array factor [13] given, respectively, by

$$f_\theta(\theta) = \left|\frac{\cos\left[\frac{\pi}{2}\cos(\theta)\right]-\cos\left(\frac{\pi}{2}\right)}{\sin(\theta)}\right|^2 \frac{\sin(N_{ele}\psi/2)}{N_{ele}\sin(\psi/2)}, \quad (7)$$

$$f_\phi(\phi) = \frac{1+\cos(\phi)}{2}, \quad (8)$$

$$F_{aa}^{norm} = \frac{1}{N_{ele}}\left(\frac{\sin(N_{ele}\psi/2)}{\sin(\psi/2)}\right), \quad (9)$$

The function representing the distance dependency of the electric field, $f_d(d)$, is given by

$$f_d(d)_{[\mathrm{m}^{-1}]} = \begin{cases} \frac{C_{2[\mathrm{m}]}}{d_{t[\mathrm{m}]}^2} + \frac{C_1}{d_{t[\mathrm{m}]}} + C_{0[\mathrm{m}^{-1}]}, & R_{rnf} < d < R_{ff} \\ \frac{1}{d_{[\mathrm{m}]}}, & d \geq R_{ff} \end{cases}, \quad (10)$$

Considering

$$E(\theta,\phi,d_l) \cong E_{lim}, \quad (11)$$

where d_l is the compliance distance and E_{lim} is the electric field limit. The compliance distance is then given by

$$d_{l[\mathrm{m}]} \cong \frac{2C_{2[\mathrm{m}]}}{-C_1 \pm \sqrt{{C_1}^2 - 4C_2\left(C_{0[\mathrm{m}^{-1}]} - \alpha\right)}}, \quad (12)$$

Where α is the ratio between the electric field limit and the maximum voltage multiplied by normalized 3D antenna radiation pattern, given by:

$$\alpha_{[\mathrm{m}^{-1}]} = \frac{E_{lim[\mathrm{V/m}]}}{V_{M[\mathrm{V}]}\, f_{\theta\phi}(\theta,\phi)}, \quad (13)$$

In the direction of maximum radiation, one has the maximum gain, i.e., $\max\{ f_{\theta\phi}(\theta,\phi)\} = 1$. Hence, in this case, the determined distance corresponds to the front border of the exclusion zone, D_{front}. The dimensions of the exclusion zone for the remaining directions can be determined by applying correction factors to the maximum antenna gain according to the antenna radiation patterns.

The power density limit, S_{lim}, is given by

$$S_{lim} = \frac{S_{\mathrm{ref}}(t)}{T_{var}(t)}, \quad (14)$$

where S_{ref} is the power density reference level established by ICNIRP and T_{var} is the temporal variation contribution.

Since the region under study is the transition between the radiating near-field and far-field regions, it is possible to consider the electric and magnetic fields directly interrelated by Z_0, according to

$$S = \frac{E^2}{120\,\pi}, \quad (15)$$

Therefore, E_{lim} can be given by:

$$E_{\mathrm{lim}} = \sqrt{120\,\pi\, S_{lim}}, \quad (16)$$

Factors such as BS usage, downlink duty cycle and spatial distribution of users should be considered in order to determine the temporal variation contribution to the variation of the EIRP and, consequently, of the electric field strength. Hence, the temporal variation contribution may be given by

$$T_{var}(t) = N_{RB}^{aloc,DL}\, \frac{N_{users}^{beam}}{N_{users}}\, F_{TDD}, \quad (17)$$

In multiband networks, such as the case under study, it is important to understand if the exposure effects add up. Therefore, the compliance distance must be determined for the case where antennas for multiple bands are allocated, and all the different spectrum bands are active. In this work, one can consider the BS antennas as the only source of radiation since, in comparison, the remaining sources do not have as much impact inside the exclusion zone. Hence, only the frequencies in use in the BSs should be considered for the exposure computation. Based on [8] and considering the reference values as well as the frequencies under study, one has

$$S_{norm}^{tot}(d) = \sum_{i=1}^{N_{bands}} \left(\frac{S_{final,i}(d)}{S_{ref,i}} \right) \leq 1, \quad (18)$$

where $S_{nomr}^{tot}(d)$ is the total normalised power density, N_{bands} is the number of active bands, $S_{final,i}(d)$ is the power density function for the i^{th} communication system, and $S_{ref,i}$ is the power density ICNIRP reference level at frequency i.

The exclusion zone front boarder, corresponding to the distance of maximum radiation, D_{front}, is such that the total normalised power density is equal to 1. The model developed and presented in [7] is used to calculate the exposure for GSM, UMTS, LTE, and NR at 700 MHz, i.e., for passive antennas.

IV. Results Analysis

A. Scenarios Description

First, the computation of the exclusion zone takes the NR 3.6 GHz as the only active system. Later, the exclusion zone without NR (W/O NR), i.e., considering all systems to be active except for NR, as well as with NR (W NR), i.e., the exclusion zone considering all systems to be active including NR, is determined.

One should notice that there are two different types of beams: the broadcast beam, always on air, and the traffic beams for user data, only on air when there is data to be exchanged (usually high gain narrow beams). According to [14], the broadcast beam has an associated power equal to 19 dBm (0.08 W), hence, due to this very low power, only traffic beams are taken into consideration for the computation of exclusion zones.

Regarding NR, for all of the defined scenarios, the frequency in use is 3.6 GHz, the input power of the antenna, P_{in}, is equal to 240 W, the maximum antenna gain, G_M is equal to 25 dBi, and the maximum number of RBs is 273, considering the 100 MHz BS bandwidth, which corresponds to a SCS equal to 30 kHz [15]. A realistic F_{TDD} value of 0.75 is considered.

It is possible to assume appropriate values for the temporal variation contribution based on previous studies conducted by means of simulations and statistical analysis. These studies give the percentage of the maximum transmit power per beam considering the 95th percentile, all of them having highly agreeing results. While it is not advisable to use the maximum output power of the antenna due to interference and EMF exposure, it may be appropriate to do so in the case where the BS is only serving one user and the maximum power may allow better service results. However, in this case, special attention must be paid to the resulting increased EMF exposure.

Of all the works published in the literature, [4] is the one that gathers the best conditions regarding the goal of this thesis while also providing values for different types of environments, user distributions and system usage, making it suitable for most general cases. In [4], the estimation of the BS usage is based on the number of simultaneous users served by the system at a specific time instant (system described using an M/M/1 queue). For the DL/UL transmission configuration, an F_{TDD} value of 0.75 has been assumed as a reasonable value for 5G. Since the maximum exposure is usually obtained when focused beams are used (LOS scenario), this is the case considered in this thesis. A 5G BS designed to cover $\pm 60^{\circ}$ in azimuth and $\pm 15^{\circ}$ in elevation is assumed.

Four User Distribution Scenarios (UDS) are defined in [4]. Urban_a considers an urban environment with a density of users uniformly distributed in azimuth and elevation. Urban_b is based on an urban environment with the highest density of users in the centre of both the azimuthal and elevation Scan Range (SR) where the variation in elevation is chosen to reflect a larger density of users in the horizontal plane. The density of users is weighted by a cosine function in azimuth and a squared cosine distribution in elevation. Rural_a considers a rural environment with a density of users uniformly distributed in azimuth and no elevation scanning employed. Finally, Rural_b also takes into

account a rural environment but with a higher density of users in the centre of the azimuthal SR, weighted by a cosine function in azimuth and no elevation scanning employed. Since, in [4], only percentages for urban and rural environments were provided, an average between the values of those two environments was considered for the suburban one. The distribution of users, the number of served independent users during the averaging time, the system usage and the fact that the results were determined for an 8×8 array antenna with an element spacing of $\lambda/2$, using a model developed to be used in the far-field will have an influence on the conservativeness of the model.

According to [4], the maximum values for EMF exposure were found to occur for very large degrees of system usage. However, in practice, usage levels close to 100% are unrealistic since this may lead to a decrease in the quality of service. The described scenarios along with the correspondent percentage of the maximum transmit power per beam (considering the 95th percentile) for two different system usage levels are presented in Table I.

TABLE I. PERCENTAGE OF MAXIMUM TRANSMIT POWER BEAM FOR THE DIFFERENT SCENARIOS AND SYSTEM USAGE.

Scenarios	Percentage of the maximum transmit power/beam (95th percentile) [%]	
	System usage [%]	
	50	95
Urban_a	2.50	7.00
Urban_b	5.00	13.00
Suburban_a	4.25	11.00
Suburban_b	6.50	17.50
Rural_a	6.00	15.00
Rural_b	8.00	22.00

Since the duration of EMF exposure has a direct impact on the reference level for exposure, it is necessary to choose appropriate values for the duration of exposure when computing the exclusion zone. Different averaging times are set, corresponding to different reference levels based on the ICNIRP guidelines. The power density reference levels for the different systems considering averaging times equal to 1 min, 6 min and 30 min, based on [8], are presented in Table II.

TABLE II. POWER DENSITY REFERENCE LEVELS FOR THE DIFFERENT SYSTEMS, AVERAGED OVER 1 MIN, 6 MIN AND 30 MIN.

System	S_{ref} [W/m^2]		
	Averaging Time [min]		
	1	6	30
NR700	NA	17.47	3.82
LTE800	NA	18.51	4.08
GSM/UMTS900	NA	20.97	4.72
LTE1800	NA	37.17	9.18
UMTS/LTE2100	NA	40.00	10.00
LTE2600	NA	40.00	10.00
NR3600	98.00	40.00	10.00

One should note that "NA" means that the entity does not need to be taken into account when determining the results for the different scenarios.

In order to study the exposure with several active systems, 9 different outdoor scenarios were established (3 in each environment, i.e., urban, suburban and rural). The definition of these scenarios is based not only on NR active antennas but also on the typical antennas installed previous to the implementation of NR. Hence, it is possible to determine the variation of the exclusion zone region before and after de NR installation on the BSs. The different scenarios along with the active mobile communication systems and frequency bands are presented in Table III.

TABLE III. MOBILE COMMUNICATIONS SYSTEMS IN EACH SCENARIO (BASED ON [7]).

Scenarios	Mobile Communications Systems Frequency Bands								
	GSM	UMTS		LTE				NR	
	900	900	2100	800	1800	2100	2600	700	3600
Urban 1	×		×		×				×
Urban 2	×		×	×			×		×
Urban 3	×		×		×		×	×	×
Suburban 1	×	×	×	×	×				×
Suburban 2	×	×		×		×		×	
Suburban 3	×		×	×	×	×		×	×
Rural 1	×	×		×				×	
Rural 2	×	×	×			×		×	
Rural 3	×	×	×	×		×		×	×

For each of the mobile communication systems, the output power per carrier and MIMO element as well as the number of MIMO elements for each LTE and NR band are based on [7].

While, for NR3600, the AAUxxxxw active antenna is taken, for GSM, UMTS, LTE and NR700, a single passive antenna should be considered, the ASIxxxxxxxx6 [16].

Since the number of carriers, N_c, used in a system may be different for different BSs installations, the exclusion zone distances corresponding to the broadside direction, D_{front}, should be determined taking into consideration different carrier configurations. Hence, in order to obtain a wide variety of results, four different configurations ($N_{c\,GSM900}/N_{c\,UMTS}$) are defined: 1/1, 2/1, 4/2 and 4/4. One should note that $N_{c\,UMTS}$ is referring to the number of carriers for all of the UMTS bands. The number of carriers and the level of MIMO must be accounted for in the input power of the antenna. This generates more conservative results since maximum transmitting powers are being assumed with a direction of maximum radiation equal for different carriers and different MIMO beams.

B. D_{front} Variation

D_{front} when only NR is active in the BS is presented in Table IV for the Urban_a, Suburban_a and Rural_a scenarios, considering a system usage of 50% and 1 min, 6 min and 30 min as averaging times. Results for other scenarios, as well as system usage and averaging times, were determined, however, since the model is not very sensitive to these variations, only a representative sample of the results is shown.

The electric field decay with distance was exclusively determined based on the simulation of an active antenna with 96 active elements, for the direction of maximum radiation. Hence, the results are based on large antennas with high gains and input powers, leading to somewhat overestimated results since subarrays and other beam directions are not being taken into account. In the model, power, gain, and other parameters defining the different scenarios lie inside a fourth root, which

condemns the variations of these parameters to be quite attenuated.

TABLE IV. D_{Front} FOR URBAN, SUBURBAN AND RURAL SCENARIOS WITH NR3600 AS THE ONLY ACTIVE SYSTEM IN THE BS.

Scenario	T_{avg} [min]	D_{Front} [m]
Urban	1	16.12
	6	16.28
	30	16.43
Suburban	1	16.23
	6	16.35
	30	16.46
Rural	1	16.28
	6	16.39
	30	16.48

Taking the multi-band exposure, an averaging time of 30 min and a system usage of 50%, the results taking 100% of the maximum transmit power per beam for the 1/1 carrier configuration and taking the actual percentage of the maximum transmit power per beam of each scenario, for each carrier configuration, are presented in Figures 10, 11, 12, 13 and 14.

Taking 100% of the maximum transmit power per beam, it is possible to conclude that the increase in the compliance distance due to the installation of NR ranges from 92.4% to 314.4% (urban scenarios), from 17.3% to 191.8% (suburban scenarios) and from 16.4% to 234.2% (rural scenarios). However, when the actual percentage of the maximum transmit power per beam of each scenario is taken, the increase in the compliance distance due to the installation of NR ranges from 24.3% to 170.4% (urban scenarios), from 16% to 78% (suburban scenarios) and from 16.4% to 104.1% (rural scenarios), showing a decrease in the compliance distance when considering actual maximum transmit powers.

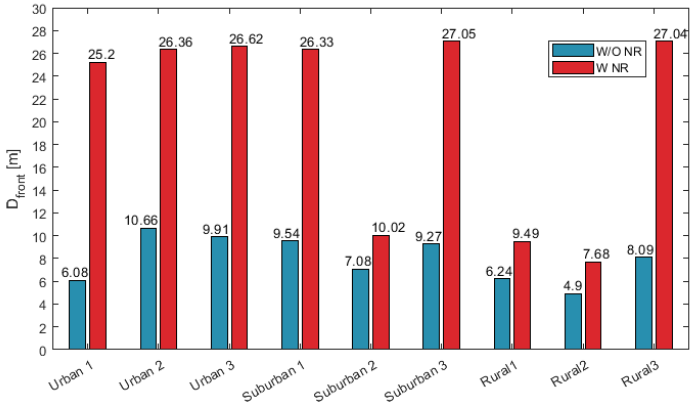

Figure 10. D_{front} for the carrier configuration 1/1 taking 100% of the maximum transmit power/beam.

The compliance distance taking the multi-band exposure with all active systems is almost the same as the one obtained when considering NR at 3.6 GHz as the only active system, since, at the computed distance, the legacy systems do not have such an impact because of their lower gains and input powers. On top of that, at that distance, almost every system is within the near-field region, excluding the LTE1800, UMTS2100, and LTE2100, which cause the field to decay much faster with distance than it would in the far-field region.

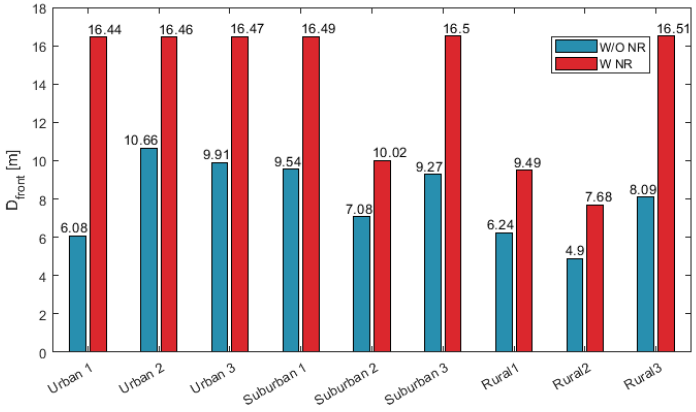

Figure 11. D_{front} for the carrier configuration 1/1 taking the actual percentage of the maximum transmit power/beam of each scenario.

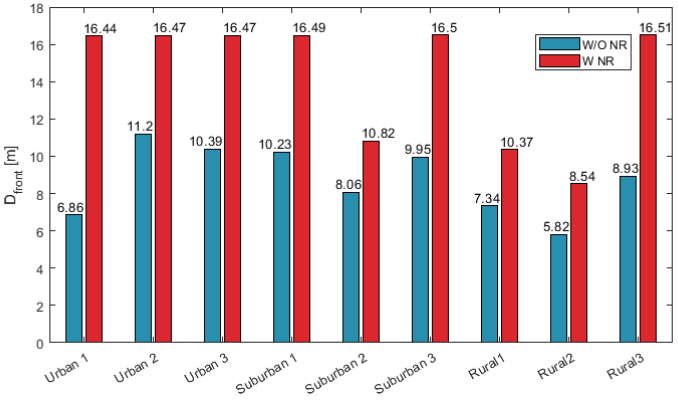

Figure 12. D_{front} for the carrier configuration 2/1 taking the actual percentage of the maximum transmit power/beam of each scenario.

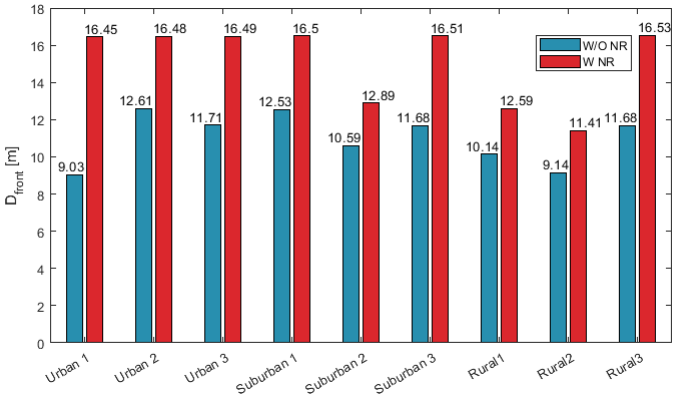

Figure 13. D_{front} results for the carrier configuration 4/2 considering the actual percentage of the maximum transmit power/beam of each scenario.

Results show that the contribution of NR3600 to D_{front} is significantly higher than the contribution of each legacy system individually. The lowest contribution of NR3600 is 13.8%, which corresponds to 86.2% of the total contribution distributed amongst the legacy systems.

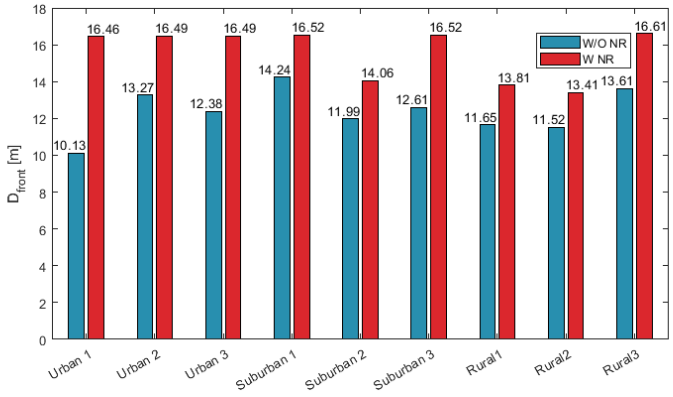

Figure 14. D_{front} results for the carrier configuration 4/4 considering the actual percentage of the maximum transmit power/beam of each scenario.

Because of the unaltered radio configuration of NR700 and NR3600 throughout the different scenarios, a lower D_{front} increase is expected when installing the NR in BSs with a higher transmitting power from legacy systems, which happens in all scenarios. Therefore, the EMF influence of NR decreases as the influence of the legacy systems increases.

The increase in D_{front} is overall lower for the scenarios that only consider the deployment of NR700, as opposed to the environments where NR3600 is installed, since NR700 works with passive antennas, having transmitted powers and antenna gains significantly lower than the ones used in NR3600.

One should notice that the scenarios with the highest total transmitted power are not always the ones producing the highest compliance distances. Lower exposure limits are set for lower frequency systems (below 2 GHz), therefore, it is expected that scenarios working with lower bands produce higher compliance distances [8].

Due to the high compliance distances obtained, some considerations should be taken regarding the public exposure in urban scenarios. For scenarios where the antennas are installed close to the ground, physical barriers may need to be installed at street level. For suburban and rural scenarios, the typical BS height for these environments should be enough to ensure the safety of the population. It was determined that physical barriers at ground level are not required in urban scenarios BSs for antennas with a height greater than 9.79 m. Uroof scenarios may also generate overexposure if an antenna is installed on top of small buildings less than 9.79 m above ground. One should also take into account the impact of D_{front} on the buildings in front of the BS, since they may be inside the exclusion zone of that BS. Assuming a common sidewalk, the width of the street would be only 11.5 m, which is quite below the 16.44 m obtained for the Urban 1 scenario with the 1/1 carrier configuration [17].

C. *Exclusion Zone Variation for Other Directions*

CST simulations for other directions was not possible due to requirements of higher machine-level capabilities, thus, radiation patterns were used instead, in order to define a somewhat accurate exclusion zone (avoiding taking the maximum power for all directions). However, since radiation patterns are determined based on far-field distances and maximum beam coverage scope is being taken, an overestimation of the results is inevitable.

In order to compute the exclusion zone limit distances for the back, side, top and bottom directions, the absolute value of the normalised gain for each direction is subtracted from the maximum antenna gain for each system. The angles corresponding to these directions are 180º for back (H plane), 90º and 270º for side (H plane), 0º for top (V plane) and 180º for bottom (V plane). The results are presented in Table V.

TABLE V. D_{back}, D_{side}, D_{top} AND D_{bottom} RESULTS FOR URBAN, SUBURBAN AND RURAL SCENARIOS WITH NR3600 AS THE ONLY ACTIVE SYSTEMS IN THE BS.

Scenario	T_{avg} [min]	D_{back} [m]	D_{side} [m]	D_{top} [m]	D_{bottom} [m]
Urban	1	3.97	15.69	3.97	3.97
	6	5.66	16.00	5.66	5.66
	30	8.61	16.28	8.61	8.61
Suburban	1	4.94	15.89	4.94	4.94
	6	6.77	16.13	6.77	6.77
	30	9.73	16.35	9.73	9.73
Rural	1	5.62	16.00	5.62	5.62
	6	7.50	16.20	7.50	7.50
	30	10.42	16.39	10.42	10.42

The distances for other directions are lower than the distances obtained for the direction of maximum radiation, as expected. However, for instance, the normalised gain used to obtain D_{Back} relies on the assumption that the radiating lobe is pointing in the opposite direction to the main radiation direction, which is a conservative approach. In addition to the fact that the use of the radiation patterns itself generates conservative results, since these patterns are determined in the far-field region, from observation of Figure 9 one can conclude that, while for the vertical beam scanning, the area corresponding to the maximum beam coverage scope agrees with the area of actual operation of an active antenna (60º), for the horizontal beam scanning the area of actual operation of the antenna is lower (120º), since the sectorization of the BS is being considered. This leads to a low significance of the obtained results. Thus, these results must be taken, keeping in mind the conservative approaches behind their computation and the actual operating scope of the AA.

Due to the low significance of the values obtained for these directions, the analysis of the exclusion zone variation for other directions when all systems are active is left out of the scope of this work.

V. CONCLUSIONS

The main goal of this thesis was to develop a model to determine EMF exposure in the vicinity of BSs antennas with 3.6 GHz NR installed in order to compute realistic exclusion zones that would guarantee the general public safety.

For Urban_a, Suburban_a and Rural_a scenarios, taking a system usage of 50% and 1 min, 6 min and 30 min as averaging times, D_{front} ranged from 16.12 m (urban scenario) to 16.48 m (rural scenario), being higher in rural scenarios, as expected.

Then, for multi-band scenarios, taking 100% of the maximum transmit power per beam, the increase in the compliance distance due to the installation of NR ranged from 92.4% to 314.4% (urban scenarios), from 17.3% to 191.8% (suburban scenarios) and from 16.4% to 234.2% (rural scenarios). However, when the actual percentage of the

maximum transmit power per beam is taken, the increase in compliance distance due to the installation of NR ranges from 24.3% to 170.4% (urban scenarios), from 16% to 78% (suburban scenarios) and from 16.4% to 104.1% (rural scenarios). The obtained results show a decrease in the compliance distance when considering actual maximum transmit powers.

The results obtained for the exclusion zone with NR are quite lower than those obtained in [7], where the increase in the compliance distance due to the installation of NR ranges from 92.3% to 248.7% (urban scenarios), from 17.3% to 131.6% (suburban scenarios) and from 14.3% to 56.4% (rural scenarios). This reduction in the exclusion zone can be explained by the use of the actual maximum transmitted power.

In order to obtain a complete exclusion zone, other directions were analysed, such as the back, side, top and bottom. However, one should take these results carefully, keeping in mind the conservative approaches behind their computation and the actual operating scope of an AA.

Although the obtained exclusion zone distances should be seen only as an approximation, the installation of the antennas should be studied with care. One should also take into account the future BS sharing between operators, where the same infrastructure will be shared by several operators, increasing the EMF exposure.

For future work, it would be interesting to take advantage of the beamforming properties of the AAs by simulating several different configurations of subarrays as these configurations would certainly make use of lower antenna input powers and gains, resulting in lower exposure levels and exclusion zone distances. A study on the influence of BS sharing between operators would also be quite interesting in order to understand its impact on EMF exposure.

REFERENCES

[1] Huawei, *New 5G, New Antenna*, White Paper, Huawei Technologies, Shenzhen, China, 2019 (https://carrier.huawei.com/~/media/CNBGV2/download/products/antenna/New-5G-New-Antenna-5G-Antenna-White-Paper-v2.pdf).

[2] Thales, https://www.thalesgroup.com/en/markets/digital-identity-and-security/mobile/inspired/5G, Oct. 2020.

[3] P. Baracca, A. Weber, T. Wild and C. Grangeat, "A statistical approach for RF exposure compliance boundary assessment in massive MIMO systems'', in *Proc. 22nd Int. ITG Workshop Smart Antennas*, Bochum, Germany, Mar. 2018.

[4] B. Thors, A. Furuskär, D. Colombi and C. Törnevik, "Time-averaged realistic maximum power levels for the assessment of radio frequency exposure for 5G radio base stations using massive MIMO", *IEEE Access*, Vol. 5, Sep. 2017, pp. 19711-19719.

[5] D. Colombi, P. Joshi, R. Pereira, D. Thomas, D. Shleifman, B. Tootoonchi, B. Xu and C. Törnevik, "Assessment of Actual Maximum RF EMF Exposure from Radio Base Stations with Massive MIMO Antennas", in 2019 Photonics & Electromagnetics Research Symposium, Rome, Italy, June 2019.

[6] D. Colombi, P. Joshi, B. Xu, F. Ghasemifard, V. Narasaraju and C. Törnevik, "Analysis of the Actual Power and EMF Exposure from Base Stations in a Commercial 5G Network", *Applied sciences*, Vol. 10, No.15, July 2020, pp. 5280.

[7] F.C.R.M Moura, *Analysis of the Impact of EMF Restrictions on 5G Base Stations Deployment in Existing Networks*, M.Sc. Thesis, Instituto Superior Técnico, University of Lisbon, Lisbon, Portugal, 2020.

[8] ICNIRP, "Guidelines for Limiting Exposure to Electromagnetic Fields (100 kHz to 300 GHz)", *Health Physics*, Vol. 118, No. 5, Mar. 2020, pp. 483-524.

[9] C. Oliveira, C.C. Fernandes, C. Reis, G. Carpinteiro, L. Ferreira, L.M. Correia and D. Sebastião, Definition of Exclusion Zones around typical Installations of Base Station Antennas, monIT Project report, Telecommunications Institute, Lisbon, Portugal, Feb. 2005.

[10] Huawei, *AAUxxxxw Technical Specifications*, Antenna datasheet, Shenzhen, China, Mar. 2021.

[11] Dassault Systèmes, 2021 (https://www.3ds.com/products-services/simulia/products/cst-studio-suite/).

[12] Dassault Systèmes, *CST Studio Suite High Frequency Simulation*, Manual guide, Deutschland, 2019 (file:///C:/Program%20Files%20(x86)/CST%20Studio%20Suite%202020/Online%20Help/cst_studio_suite_help.htm#general/welcome_de.htm).

[13] C. A. Balanis, *Antenna Theory: Analysis and Design*, Fourth Edition, John Wiley & Sons, New Jersey, USA, 2016.

[14] Huawei, https://www.huawei.com/en/, September 2021.

[15] iTecTec, https://itectec.com/spec/5g-nr-bs-channel-bandwidth/, Aug. 2021.

[16] Huawei, ASIxxxxxxxx6 Technical Specifications, Antenna datasheet, Shenzhen, China, Dec. 2019.

[17] IMTT, Road Network - Planning and Design Principles (in Portuguese), Instituto da Mobilidade e dos Transportes Terrestres, Mar. 2011 (http://www.imt-ip.pt/sites/IMTT/Portugues/Planeamento/DocumentosdeReferencia/PacotedaMobilidade/Paginas/QuadrodeReferenciaparaPlanosdeMobilidadeAcessibilidadeeTransportes.aspx).